P412

Revised Version

CMEs, the Tail of the Solar Wind Magnetic Field Distribution, and 11-yr Cosmic Ray Modulation at 1 AU

E.W. Cliver

Air Force Research Laboratory, Space Vehicles Directorate (VSBXS),

29 Randolph Road, Hanscom Air Force Base, MA 01731-3010;

edward.cliver@hanscom.af.mil

A.G. Ling

Radex, Incorporated, 3 Preston Court, Bedford, MA 01730;

alan.ling@hanscom.af.mil

and

I. G. Richardson

Laboratory for High Energy Astrophysics (Code 661),

NASA Goddard Space Flight Center, Greenbelt, MD 20771;

richardson@lheavx.gsfc.nasa.gov

ABSTRACT

Using a recent classification of the solar wind at 1 AU into its principal components (slow solar wind, high-speed streams, and coronal mass ejections (CMEs) for 1972-2000, we show that the monthly-averaged galactic cosmic ray intensity is anti-correlated with the percentage of time that the Earth is imbedded in CME flows. We suggest that this correlation results primarily from a CME-

related change in the tail of the distribution function of hourly-averaged values of the solar wind magnetic field (B) between solar minimum and solar maximum. The number of high-B ($\geq$ 10 nT) values increases by a factor of ~3 from minimum to maximum (from 5% of all hours to 17%), with about two-thirds of this increase due to CMEs. On an hour-to-hour basis, average changes of cosmic ray intensity at Earth become negative for solar wind magnetic field values $\geq$ 10 nT.

1. INTRODUCTION

The cause of the 11-yr modulation of galactic cosmic rays has been a matter of debate since Forbush (1954, 1958) discovered that the cosmic ray intensity varied inversely with sunspot number. It was recognized early on that magnetic fields injected via solar eruptions into the interplanetary medium could account for the 11-yr variability of cosmic rays through convection/diffusion processes (e.g., Morrison 1956; Parker 1958; Lockwood 1960). Subsequently, Jokipii and colleagues (Jokipii, Levy, & Hubbard 1977; Kota & Jokipii 1983; see also: Smith & Thomas 1986; Saito & Swinson 1986) pointed out the importance of gradient/curvature drifts in the large-scale magnetic field of the heliosphere for long-term modulation. Current treatments (e.g., McDonald 1998; Potgieter 1998; Jokipii & Wibberenz 1998; Heber 2002; Heber et al. 2002) include both of these effects, with drift effects dominating at solar minimum and diffusive/convective processes primarily responsible for the low cosmic ray intensities observed at solar maximum.

Cane et al. (1999a,b) recently refocused attention on the role of the solar magnetic field for long-term modulation by emphasizing that steplike modulations were present at 1 AU (McDonald et al. 1981), before the formation of the global merged interaction regions (Burlaga, McDonald, & Ness 1993; McDonald, Lal, & McGuire 1993) at ~10 AU that produce long-lived Forbushlike decreases in the outer heliosphere. Cane et al. (1999a,b) noted that monthly averages of the solar wind magnetic field and cosmic ray intensity were anti-correlated (see also: Bieber et al. 1993; Burlaga & Ness 1998; Burlaga et al. 2002) and that certain modulation features were also present in variations of the solar open magnetic flux. They implied (by discounting the role of CMEs) that variations in the open magnetic flux might drive the 11-yr modulation cycle. Cliver & Ling (2001b) used correlations between solar data (open magnetic flux, sunspot number, and coronal mass ejection rate) and cosmic ray intensity to argue that coronal mass ejections (CMEs), which originate in closed field regions on the Sun (Hundhausen 1993), were a more likely candidate for a modulation driver. While CMEs account for only ~10% (or less) of the solar wind mass loss (Webb & Howard 1994), various authors (Bieber & Rust 1995; Low 2001) have proposed a central role for CMEs in expelling the magnetic flux and helicity generated by the dynamo during a solar cycle.

In this study, we use a recent classification by Richardson, Cane, & Cliver (2002) of the solar wind at 1 AU into its principal components (slow solar wind, high-speed streams (including corotating interaction regions), and CMEs (including shocks and post-shock flows)) for 1972-2000, to identify which solar

wind component is most closely linked to the 11-yr cosmic ray variation at 1 AU. Previous studies have focused on short-term cosmic ray intensity decreases associated with selected solar wind phenomena such as magnetic clouds and shocks (e.g., Zhang & Burlaga 1988) but have not considered the data in a synoptic fashion as we are now able to do using the classification of Richardson et al. (2002). Our analysis will focus on differences between distribution functions of solar wind *B* values for solar minimum and maximum periods. We are particularly interested in the tail of the distribution and its effects on cosmic rays since high-*B* values (□ 10 nT) have long been implicated (Barouch & Burlaga 1975) in short-term modulation effects at 1 AU.

Our analysis is presented in § 2 and the results are discussed in § 3.

2. ANALYSIS

2.1 *Solar Wind Classification*

The solar wind classification procedure is described in detail in Richardson, Cliver, & Cane (2000). A variety of signatures of interplanetary CMEs, including bi-directional solar wind heat flux electrons and energetic ions, intervals of abnormally low plasma proton temperature, geomagnetic storm sudden commencements, magnetic field rotations, and Forbush decreases were used to identify intervals of CMEs, shocks, and post-shock flows. High-speed streams were identified on the basis of corotation, sustained high-speed flows, low densities, and a predominant magnetic field polarity while the slow solar wind was characterized by speeds below ~400 km s^{-1} and high variability in the plasma parameters. Because of the inclusion of proxy (other than solar wind)

data in the classification process, the categorization of the solar wind into its three basic components is remarkably complete for the 1972-2000 interval with an overall "duty cycle" of ~95% and coverage rarely dropping below 60% for any 3-rotation interval (see Figure 3(d) in Richardson et al. 2002). Solar wind intervals not identified as one of the three basis types, either because of missing data or inconclusive signatures, are referred to as "unclear".

This solar wind classification of Richardson et al. (2000) has been used to examine solar wind sources of geomagnetic activity in several studies (Richardson et al. 2000; Richardson, Cliver, & Cane 2001; Richardson et al. 2002). Here we apply it to the question of the solar wind driver of cosmic ray modulation at 1 AU.

2.2 *Solar Cycle Variation of the Time Earth Spends in the Different Flow Types*

Figure 1 shows the fraction of time each month for 1972-2000 that the Earth was in CME flows (thin line; unclear intervals were ignored when computing percentages) and the (inverted) Climax cosmic ray intensity (thick line; plotted in 27-day averages). The solar cycle variation in the rate of CME-related structures at 1 AU reflects the 11-yr variation in the rate of CMEs at the Sun (Cliver et al. 1994; Webb & Howard 1994) obtained from coronagraph records. It can be seen in Figure 1 that the cosmic ray intensity is anti-correlated with the CME occurrence frequency at Earth ($r = -0.65$). Corresponding correlation coefficients for high-speed streams and slow solar wind are -0.37 and -0.34, respectively. Cliver & Ling (2001b) previously reported a correlation coefficient

of –0.37 between the solar open magnetic flux and Climax cosmic-ray intensity for 1967-1972.

Using the classification of Richardson et al. (2000), Cliver & Ling (2001b) reported that, on average, the Earth is embedded in CME flows (Including shocks and post-shock flows as well as CME driver gas) ~35% of the time at solar maximum versus ~10% of the time during solar minimum. Corresponding figures for the fraction of the solar wind *B* carried by CME flows are ~35-40% and ~10%. In Figure 2, this change in the structure of the solar wind and the cosmic ray response is illustrated for a representative solar minimum period (a) and at the onset of the modulation in cycle 21 (b). The gray shaded time periods, corresponding to CME flows at Earth, indicate that such flows are far more prevalent at solar maximum than at minimum. Forbush decreases are clearly associated with CMEs while intervals of high-speed streams and slow solar wind are generally associated with flat or recovering cosmic ray intensity.

In Figure 1 it can be seen that the cosmic ray intensity lags changes in CME solar wind activity at Earth in odd-numbered solar cycles. This effect was first noted by Nagashima & Morishita (1980) from a comparison of the cosmic ray curve with sunspot number and has been reported more recently using longer data sets by several others using various indicators of solar activity (Ahluwalia & Wilson 1996 (10.7 cm radio flux), Van Allen 2000 (sunspot number), Cliver & Ling 2001a (sunspot number, tilt angle of the heliospheric current sheet)). Both Van Allen (2000) and Cliver & Ling (2001a) interpreted the lag in cosmic ray responsiveness in odd-numbered cycles in terms of a 22-yr drift effect related to

the preferred direction of approach of cosmic rays to the heliosphere (from the polar direction or inward along the solar equator) dependent on the Sun's magnetic polarity.

2.3 *The tail of the distribution function of solar wind B and its variation with the solar cycle*

To investigate the cause of the correlation in Figure 1, we obtained histograms of hourly-averaged values of solar wind *B* for the various flow types for the increasing-modulation (falling cosmic ray intensity) years of cycles 21 (1978-1982), 22 (1988-1991), and 23 (partial; 1998-2000) (ignoring the drift-related decrease in 1987 (Smith 1990; cf., Cliver & Kahler 1991)). Overall solar wind *B* coverage for these combined maximum periods was 71%. Coverage was slightly higher for high-speed streams and slow solar wind (both about 82%) than for CMEs (75%). Not unexpectedly, unclears have a lower coverage rate (33%). During solar maximum years, Earth spends approximately one-third of the time in each of the three basic flow types (Richardson et al. 2002). In Figure 3 it can be seen that the tail of the solar wind *B* distribution is dominated by CMEs. (The high-speed stream *B*-value > 40 nT (on 20 Nov 1978 at 19 UT) is judged to be spurious and is eliminated from subsequent plots; it apparently results from a single ISEE-3 1-min average of ~160 nT which occurs immediately prior to a > 3 hr data gap.)

The existence of a solar minimum to solar maximum variation in high-*B* values can be seen in Figure 4. The filled circles give the *B* distribution for all

flow types (except unclears) for the combined solar maximum epochs of cycles 21, 22, and 23 (1978-1982, 1988-1991, 1998-2000) while the open circles correspond to the minimum epochs of 1975-1977, 1985-1987, and 1995-1997. (The solar minimum distribution was normalized to have the same number of points as the maximum distribution.) The "Δ" and "+" data points give the *B* distribution for CMEs for the maximum and minimum (normalized) epoch years, respectively, showing that the increase in the number of high-*B* (□ 10 nT) values from maximum to minimum (by a factor of ~3.2) is primarily (65%) due to increased CME activity. During the combined increasing-modulation intervals, 17% of all hours had average *B* values □ 10 nT vs. 5% for the three minimum epochs.

2.4 *The effect of the tail of the solar wind B distribution on cosmic ray intensity*

To gauge the effect of high-*B* values on the cosmic ray intensity, we determined the average hour-to-hour change in the Climax neutron monitor count rate as a function of *B* for solar maximum epochs (Figures 5). The procedure was to take each *B* value (excluding unclears) within a given bin, determine its associated change in cosmic ray intensity (ΔCR, current hourly average minus preceding hourly average), sum the signed differences, and divide by the number of points, plotting the value at the midpoint of the bin. We used bin sizes of 2 nT from 0-10 nT, 5 nT from 10-20 nT, and 10 nT through 50 nT (statistical error bars, given by square root (average (ΔCR)/N), where N = number of data points, are shown). No correction was made to the Climax count rate for the diurnal variation; its effect should average to zero for large data samples. For the

combined solar maximum periods considered in Figure 5, Climax cosmic ray coverage was 93% (after removal of the relatively short periods with cosmic ray increases due to ground level events (totaling ~0.1% of the data); this correction had a negligible effect on our results). From Figure 5 we see that, on average, cosmic ray intensity decreases (falls below the dashed line) for $B \lesssim 10$ nT for solar maximum periods. The solid line in the figure shows that the fraction of B values in CMEs is ~40% for B = 10 nT and increases to ~ 90% for $B \sim 25$ nT. In all, 56% of $B \geq 10$ nT values during the years considered here at the peaks of cycles 21, 22, and 23 occurred during CME flows (vs. 29% in high-speed streams and 15% in slow solar wind), with the CME percentage and the average cosmic ray decrease growing for progressively larger B values above 10 nT.

2.5 *Occurrence frequency of high-B values, 1965-2000*

Burlaga and colleagues have pointed out in several studies (e.g., Burlaga & King 1979; Burlaga & Ness 1998; Burlaga 2001) that hourly values of the solar wind B have an approximate (but not exact, Feynman & Ruzmaikin 1994) lognormal distribution. As a result, the ratio $SD(B)/\langle B \rangle$ (where $SD(B)$ is the standard deviation of B, $\langle B \rangle$ is average B, and both parameters are computed on an annual basis) is roughly constant (at ~0.6) as shown by Burlaga & Ness (1998) for individual years from 1980 through 1994. This approximately fixed ratio implies a correlation between monthly counts of ≥ 10 nT values (middle panel of Figure 6; normalized for duty cycle; 25% magnetometer coverage required) and monthly-averaged solar wind B values (top panel) for 1966-2000 ($r = 0.90$). The monthly high-B count rate is anti-correlated with monthly averages

of the Climax cosmic ray intensity (bottom panel; r = -0.61) over this period. (Cliver & Ling (2001b) obtained an identical correlation coefficient between the CME rate and the Climax cosmic ray intensity for 1979-1989.) For comparison, the correlation coefficient between monthly averages of B and the Climax cosmic ray intensity is –0.68 for 1966-2000. The slightly lower value of the correlation coefficient for the high-*B* counts is not unexpected since they account for only 11% of all *B*-values during this interval and will have a noisier time history than average *B*.

3. SUMMARY AND DISCUSSION

3.1 *Synopsis: CMEs, the Tail of the Solar Wind Magnetic Field Distribution, and Cosmic Ray Modulation*

This study of long-term cosmic ray modulation was based on the classification work of Richardson et al. (2002) which for the first time separated the solar wind for an extended period covering multiple solar cycles into its three basic components: CME-related flows (including shocks and postshock flows), high-speed streams (including interaction regions), and slow solar wind. From 1972-2000, the fraction of time Earth spent in CME flows varied from ~10% of the time at solar minimum periods to ~35% at solar maxima (Richardson et al. 2002) and was anticorrelated (r = -0.65) with the Climax cosmic ray intensity (Figure 1). (The corresponding correlation for the fraction of time Earth was imbedded in high-speed streams or low speed streams was r ~ -0.35.) The 11-yr variation in the rate of CMEs (Webb & Howard 1994; Richardson et al. 2002) accounted for 65% of a ~3-fold increase (from 5% to 17% of all hours) in hourly-averaged

values of $B \geq 10$ nT between solar minimum and solar maximum (Figures 4). For periods on the rise and at the peak of the solar cycle, hourly-averaged changes of cosmic ray intensity become negative for solar wind magnetic field values ≥ 10 nT (Figure 5). The above results lead us to suggest that the solar cycle variation of strong (≥ 10 nT) solar wind magnetic fields carried by coronal mass ejections plays a key role in the 11-yr cosmic ray modulation cycle.

Hirshberg (1969) was the first to point out the large increase in the rate of occurrence of infrequent high-*B* (3-hr averages > 8 nT) values at solar maximum in comparison with solar minimum. As Siscoe, Crooker, & Christopher (1978) noted, large changes in the tail may not strongly affect average values. For example, the increase in average field strength between the solar minimum periods and the solar maximum periods in Figure 4 was ~30% (5.6 nT to 7.4 nT) vs. the ~300% increase in the number of $B \geq 10$ nT values. We note that a *B* value of ~10 nT is approximately twice that of the average solar wind field strength at solar minimum.

An emphasis on the significance of strong field values (preferentially found in CMEs) for modulation is not new. Barouch & Burlaga (1975), in a study of data from 1968, originally noted a relationship between cosmic ray depressions at Earth and hourly-averaged > 10 nT solar wind *B* values, and Burlaga and colleagues (Burlaga & Ness 1998; Burlaga et al. 2002) have stressed the importance of strong fields in the tail of the quasi-lognormal distribution function of *B* (e.g., Burlaga & King 1979; Slavin & Smith 1983) for long-term modulation.

3.2 *Modulation During Solar Cycle 20*

Modulation during solar cycle 20 (1964-1976) presents difficulties, discussed in the following subsections, for our working hypothesis regarding the importance of the CME-dominated tail of the solar wind *B* distribution function for long-term modulation at 1 AU.

3.2.1 *Correlation Between B and Cosmic Ray Intensity*

As was pointed out by Ahluwalia (2000) and as can be seen in Figure 6, the anti-correlation between cosmic ray intensity and solar wind *B* for the maximum of cycle 20 is not compelling, for either monthly averages or □ 10 nT counts. Ahluwalia (2000) drew attention to the work of Exarhos & Moussas (1999), who calculated a magnetic field strength at the termination shock (dependent on the size of the heliosphere) for cycle 20 that was ~30% larger than that observed for cycles 21 and 22. (See Webber & Lockwood (2001a,b) for a recent comprehensive treatment of modulation beyond the termination shock.) A significant contribution to modulation from the termination shock during cycle 20 could dilute the correlation with the field at 1 AU for that cycle. Alternatively, Wibberenz, Richardson, & Cane (2002) concluded that the poor correlation between average solar wind *B* and cosmic ray intensity in cycle 20 resulted from the relatively weak drift of particles into the inner heliosphere during the ascending phase of this cycle and an unusually prolonged period of solar magnetic polarity reversal.

3.2.2 *Mini-cycles in 1973 and 1974*

The modulation "mini-cycles" superimposed on the cosmic ray maximum in 1973 and 1974 (Garcia-Munoz, Mason, & Simpson 1977) were not accompanied by strong CME activity (Wibberenz & Cane 2000; see also Cliver, Dröge, & Müller-Mellin 1993). Hewish (2001) drew attention to the "exceptionally sustained epoch of high-speed solar wind streams" emanating from the "monster" coronal holes (Hundhausen 1977) that characterized these years as a possible modulation driver for the mini-cycles (for counter-arguments to this viewpoint, see Wibberenz & Cane 2001). Ahluwalia (2003) also emphasized the importance of high-speed streams during this period and obtained a strong correlation between the product of B and v and the cosmic ray intensity. Inspection of the solar wind data for 1973-1974 indicates that the high-B values are preferentially located in the interaction regions (see Crooker & Cliver 1994) at the front of these high-speed streams. Monthly counts of $B \square 10$ nT values and the Climax cosmic ray intensity are anti-correlated at the $r = -0.53$ level during 1973-1974 ($r = -0.63$ for average B; ~10% of all hours during this interval had average $B \square 10$ nT.)

3.3 *Recent Modeling Results*

Wibberenz & Cane (2001) and Wibberenz et al. (2002) have used the average solar wind field strength to successfully model modulation during the 1973-1974 minicycles and for the multi-cycle period from 1965-2001, respectively. A key feature of the Wibberenz et al. (2002) study is a variable cosmic ray recovery time dependent on the polarity of the global solar magnetic

field. The agreement obtained between observation and theory, for a range of energies and using relatively few free parameters, is impressive. Because the number of hours per month of high-*B* values in the solar wind and the average monthly field strength of the solar wind are highly correlated (Figure 6), the modeling results of Wibberenz et al. (2002) are not inconsistent with our thesis that CMEs are important for long-term modulation at 1 AU.

3.4 *Local vs. Global Modulation*

In this study we considered the effect of solar wind restructuring between minimum and maximum on the size distribution of the IMF strength and examined the "instantaneous" cosmic ray response at Earth to hourly averaged fields of different sizes to argue that CMEs play a key role in transmitting the Sun's 11-yr modulation message. Clearly, as can be seen by the lag of the cosmic ray curve to changes in solar wind structure for odd-numbered solar cycles (Figure 1), modulation is a global phenomenon involving drift as well as diffusion processes and the cosmic ray curve at Earth is not simply due to the local phenomena investigated in this paper. The evolution of both the helisopheric current sheet (tilt angle) and the latitude distribution of CMEs need to be taken into account. Nevertheless, Earth serves as a test probe of the diffusive modulation process, and at 1 AU in the ecliptic plane it is the strong fields preferentially associated with CMEs that are "cosmic ray effective".

Acknowledgements. We thank Len Burlaga for helpful discussions and the referee for helpful comments. AGL's work was supported by AFRL contract F19628-00-C-0089.

References

Ahluwalia, H.S. 2000, Geophys. Res. Lett., 27(11), 1603

Ahluwalia, H.S. 2003, Geophys. Res. Lett., 30 (3), 1133, doi:10.1029/2002GL016017

Ahluwalia, H.S., & Wilson, M.D. 1996, J. Geophys. Res., 101, 4879

Bieber, J.W., Chen, J., Matthaeus, W.H., Smith, C.W., & Pomerantz, M.A. 1993, J. Geophys. Res., 98, 3585

Bieber, J.W., & Rust, D.M. 1995, Astrophys. J., 453, 911

Barouch, E., & Burlaga, L.F. 1975, J. Geophys. Res., 80, 449

Burlaga, L.F. 2001, J. Geophys. Res., 106, 15,917

Burlaga, L.F., & King, J.H 1979, J. Geophys. Res., 84, 6633

Burlaga, L.F., McDonald, F.B., & Ness, N.F. 1993, JGR, 98, 1

Burlaga, L.F., & Ness, N.F. 1998, J. Geophys. Res., 103, 29,719

Burlaga, L.F., Ness, N.F., McDonald, F.B., Richardson, J.D., & Wang, C. 2002, Astrophys. J. (submitted)

Cane, H.V., Wibberenz, G., & Richardson, I.G. 1999a, in AIP Conf. Proc. 471, Solar Wind 9, ed. S.R. Habbal, R. Esser, J.V. Hollweg, & P.A. Isenberg (New York: AIP), 99

Cane, H.V., Wibberenz, G., Richardson, I.G., & von Rosenvinge, T.T. 1999b,

Geophys. Res. Lett., 26(5), 565

Cliver, E., & Kahler, S. 1991, Proc. 22nd Int. Cosmic Ray Conf., 3, 410

Cliver, E.W., Dröge, W., & Müller-Mellin, R. 1993, J. Geophys. Res., 98, 15,231

Cliver, E.W., St. Cyr, O.C., Howard, R.A., & McIntosh, P.S. 1994, in Solar Coronal Structures, IAU Colloq. 144, eds., V. Rusin, P. Heinzel, & J. Vial (Bratislava, Slovakia: Veda), 83

Cliver, E.W., & Ling, A.G. 2001a, Astrophys. J. Lett., 551, L189

Cliver, E.W., & Ling, A.G. 2001b, Astrophys. J., 556, 432

Crooker, N.U., & Cliver, E.W. 1994, J. Geophys. Res., 99, 23,383

Exarhos, G., & Moussas, X. 1999, Solar Phys., 187, 157

Feynman, J., & Ruzmaikin, A. 1994, J. Geophys. Res., 99, 17,645

Forbush, S.E. 1954, J. Geophys. Res., 59, 525

Forbush, S.E. 1958, J. Geophys. Res., 63, 651

Garcia-Munoz, M., Mason, G.M., & Simpson, J.A. 1977, Astrophys. J., 213, 263

Heber, B. 2002, in Proc. 27th Int. Cosmic Ray Conf.: Invited, Rapporteur, and Highlight Papers (in press)

Heber, B., et al. 2002, J. Geophys. Res., 107, No. A10, 1274, doi:10.1029/2001JA000329,2002

Hewish, A. 2001, J. Geophys. Res., 106, 29,409

Hirshberg, J. 1969, J. Geophys. Res., 74, 5814

Hundhausen, A. J. 1977, in Coronal Holes and High Speed Wind Streams, ed., J.B. Zirker, (Boulder, CO: Colorado Associated University Press), p. 225

Hundhausen, A.J. 1993, J. Geophys. Res., 98, 13,177

Jokipii, J.R., Levy, E.H., & Hubbard, W.B. 1977, Astrophys. J., 213, 861

Jokipii, J.R., & Wibberenz, G. 1998, Space Sci. Rev., 83, 365

Kota, J., & Jokipii, R. 1983, Astrophys. J., 265, 573

Lockwood, J.A. 1960, J. Geophys. Res., 65, 19

Low, B.C. 2001, J. Geophys. Res., 106, 25,141

McDonald, F.B. 1998, Space Sci. Rev., 83, 33

McDonald, F.B., Lal, N., Trainor, J.H., Van Hollebeke, M.A.I., & Webber, W.R. 1981, Astrophys. J. Lett., 249, L71

McDonald, F.B., Lal, N., & McGuire, R.E. 1993, J. Geophys. Res., 98, 1243

Morrison, P. 1956, Phys. Rev., 101, 1347

Nagashima, K., & Morishita, I. 1980, Planet. Space Sci., 28, 195

Parker, E.N. 1958, Phys. Rev., 110, 1445

Osherovich, V.A., Fainberg, J., & Stone, R.G. 1999, Geophys. Res. Lett., 26(16), 2597

Potgieter, M.S. 1998, Space Sci. Rev., 83, 147

Richardson, I.G., Cliver, E.W., & Cane, H.V. 2000, J. Geophys. Res., 105, 18,203

Richardson, I.G., Cliver, E.W., & Cane, H.V. 2001, Geophys. Res. Lett., 28, 2569

Richardson, I.G., Cane, H.V., & Cliver, E.W. 2002, J. Geophys. Res., 107, 10.1029/2001JA000504

Richardson, I.G., Wibberenz, G., & Cane, H.V. 1996, J. Geophys. Res., 101,

13,483

Saito, T., & Swinson, D.B. 1986, J. Geophys. Res., 91, 4536

Siscoe, G.L., Crooker, N.U., & Christopher, L. 1978, Solar Phys., 56, 449

Slavin, J.A., & Smith, E.J. 1983, Solar Wind Five, ed., M. Neugebauer, NASA Conf. Pub. CP-2280, p. 323

Smith, E.J. 1990, J. Geophys. Res., 95, 18,731

Smith, E.J., & Thomas, B.T. 1986, J. Geophys. Res., 91, 2933

Van Allen, J.A. 2000 Geophys. Res. Lett., 27, 2453

Webb, D.F., & Howard, R.A. 1994, J. Geophys. Res., 99, 4201

Webber, W.R., & Lockwood, J.A., 2001a, J. Geophys. Res., 106, 29,323

Webber, W.R., & Lockwood, J.A., 2001b, J. Geophys. Res., 106, 29,333

Wibberenz, G., & Cane, H.V. 2000, J. Geophys. Res., 105, 18,315

Wibberenz, G., & Cane, H.V. 2001, J. Geophys. Res., 106, 29,413

Wibberenz, G., Richardson, I.G., & Cane, H.V. 2002, J. Geophys. Res. (in press)

Zhang, G., & Burlaga, L.F. 1988, J. Geophys. Res., 93, 2511

Figure Captions

Figure 1 Fraction of time that the Earth was imbedded in CME flows each month (thin line) compared with 27-day rotation averages of the (inverted) Climax cosmic ray intensity (thick line) from January 1972 – July 2000. Solar cycle numbers are given at the bottom of the figure.

Figure 2 Climax neutron monitor intensity for (a) a solar minimum period and (b) for a solar maximum period. Intervals of the three basic flow types in the solar wind are indicated. CME = coronal mass ejections (including shocks and post shock flows); HSS = high-speed streams; SSW = slow solar wind. A thick bar at the bottom of an interval indicates an unclear solar wind classification. Daily averages of the Climax cosmic ray intensity are shown for each interval.

Figure 3 Distributions of solar wind *B* (hourly averages) for the three basic flow types for the increasing-modulation years of cycles 21 (1978-1982), 22 (1988-1991; see text), and 23 (1998-2000).

Figure 4 Solar wind *B* distributions (hourly averages) for: all solar wind types (excluding "unclears") during increasing-modulation years (filled circles: 1978-1982 + 1988-1991 + 1998-2000); all solar wind types during minimum modulation years (open circles: 1975-1977 + 1985-1987 + 1995-1997); CMEs for increasing-modulation years (triangles); and CMEs for minimum modulation years (plus signs). The combined minimum solar wind distribution (all flow types) was normalized to have

the same number of points as the corresponding maximum distribution, and the minimum CME distribution was adjusted accordingly.

Figure 5 Average hour-to-hour change in the Climax cosmic ray count rate (filled circles) as a function of *B* for all flow types combined for the increasing-modulation years of cycles 21 (1978-1982), 22 (1988-1991), and 23 (1998-2000). The dashed-line is drawn at zero change in cosmic ray intensity and the thin curve gives the fraction of hours that Earth was in CME flows as a function of *B*. Statistical error bars are shown.

Figure 6 Top panel. Monthly averages of solar wind *B* for 1966-2000. Middle panel. Monthly counts (duty-cycle corrected) of the number of occurrences of $B \geq 10$ nT in hourly solar wind averages for 1966-2000. Bottom panel. Monthly averages of the Climax neutron monitor counting rate for 1966–2000. Correlation coefficients are given for comparisons of the parameters in the top and bottom panels with the annual counts of high-*B* values in the middle panel.

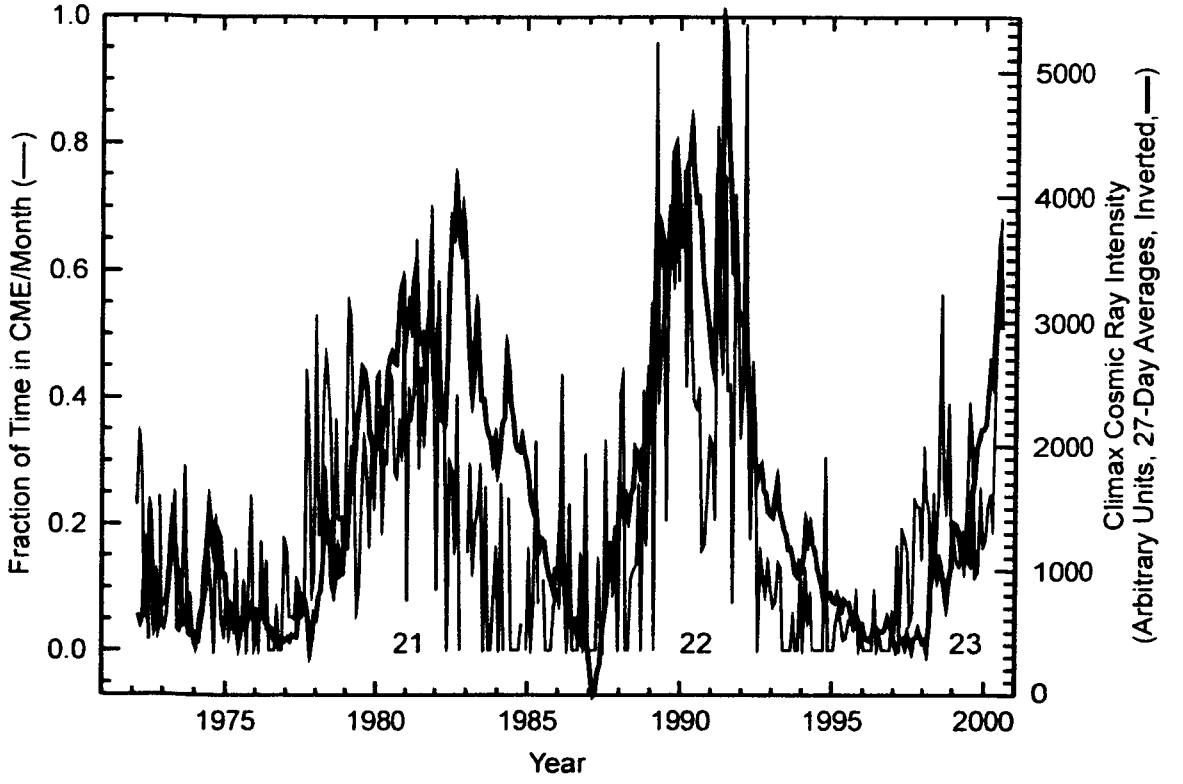

Figure 1

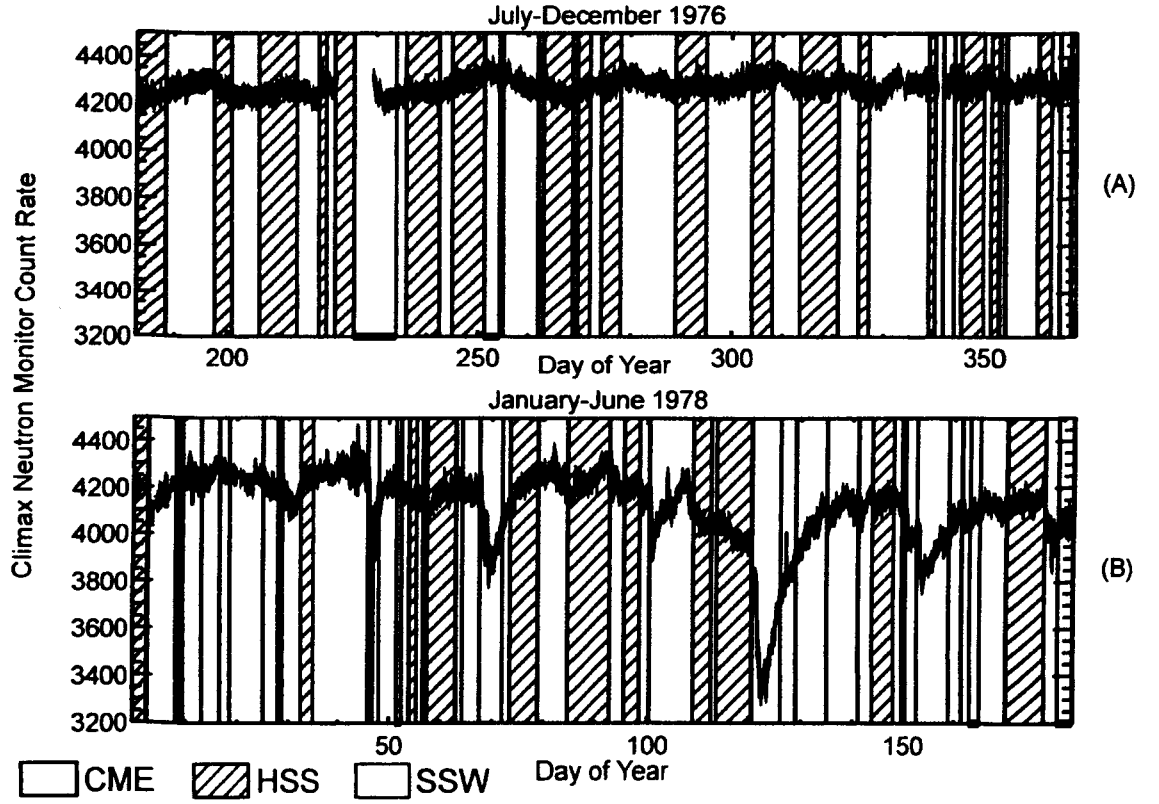

Figure 2

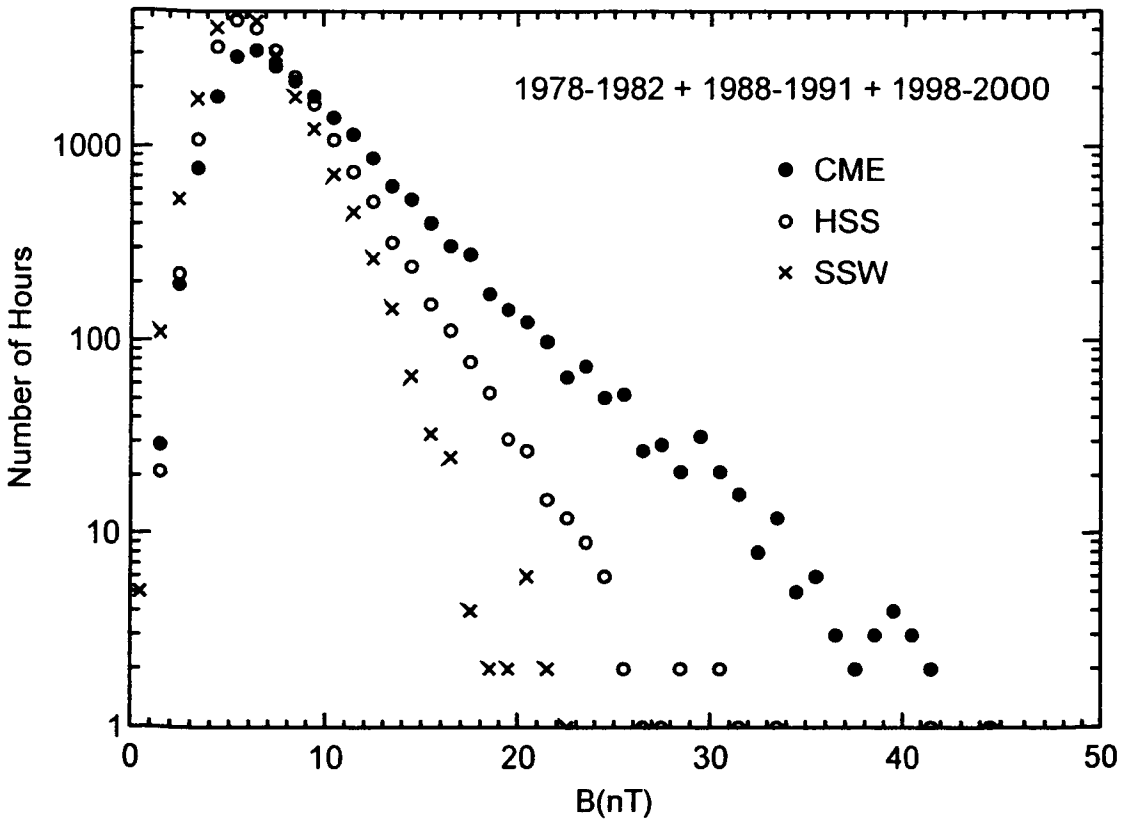
1978-1982 + 1988-1991 + 1998-2000
CME
HSS
SSW
Number of Hours
1000
100
10
1
0
10
20
30
40
50
B(nT)

Figure 3

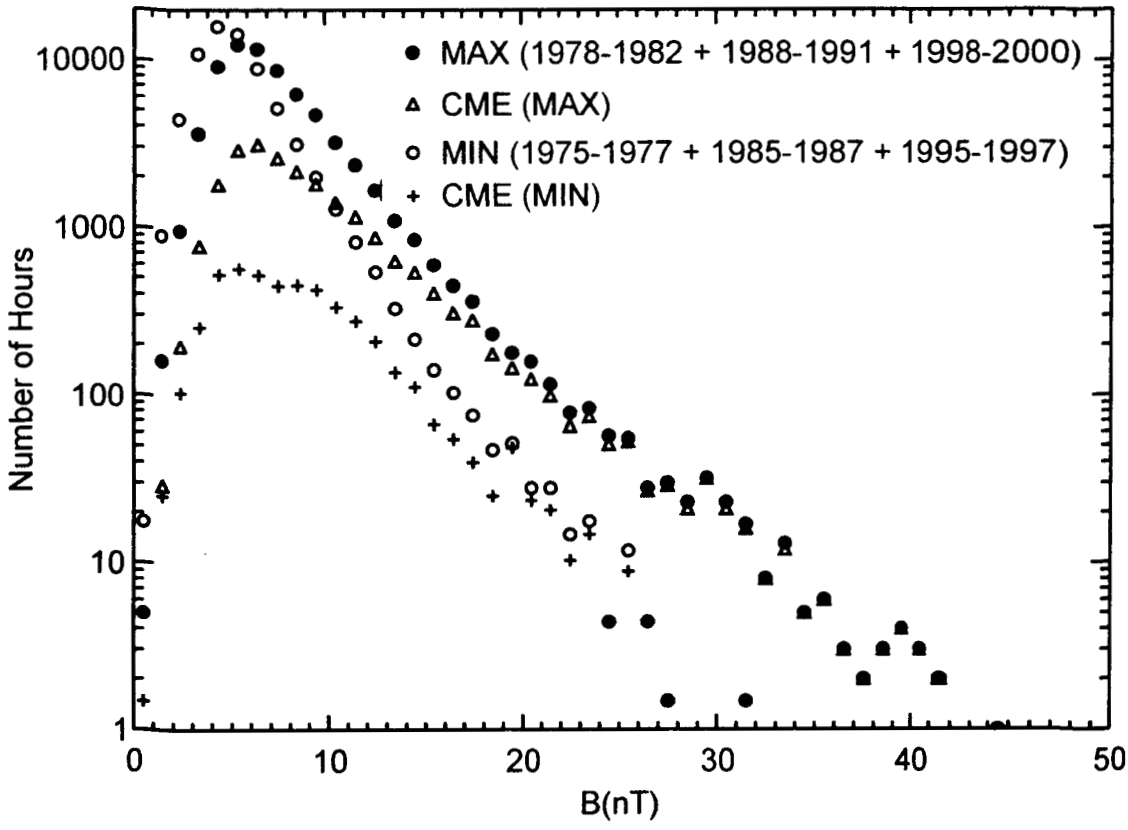
MAX (1978-1982 + 1988-1991 + 1998-2000)
CME (MAX)
MIN (1975-1977 + 1985-1987 + 1995-1997)
CME (MIN)
Number of Hours
B(nT)
10000
1000
100
10
1
0
10
20
30
40
50

Figure 4

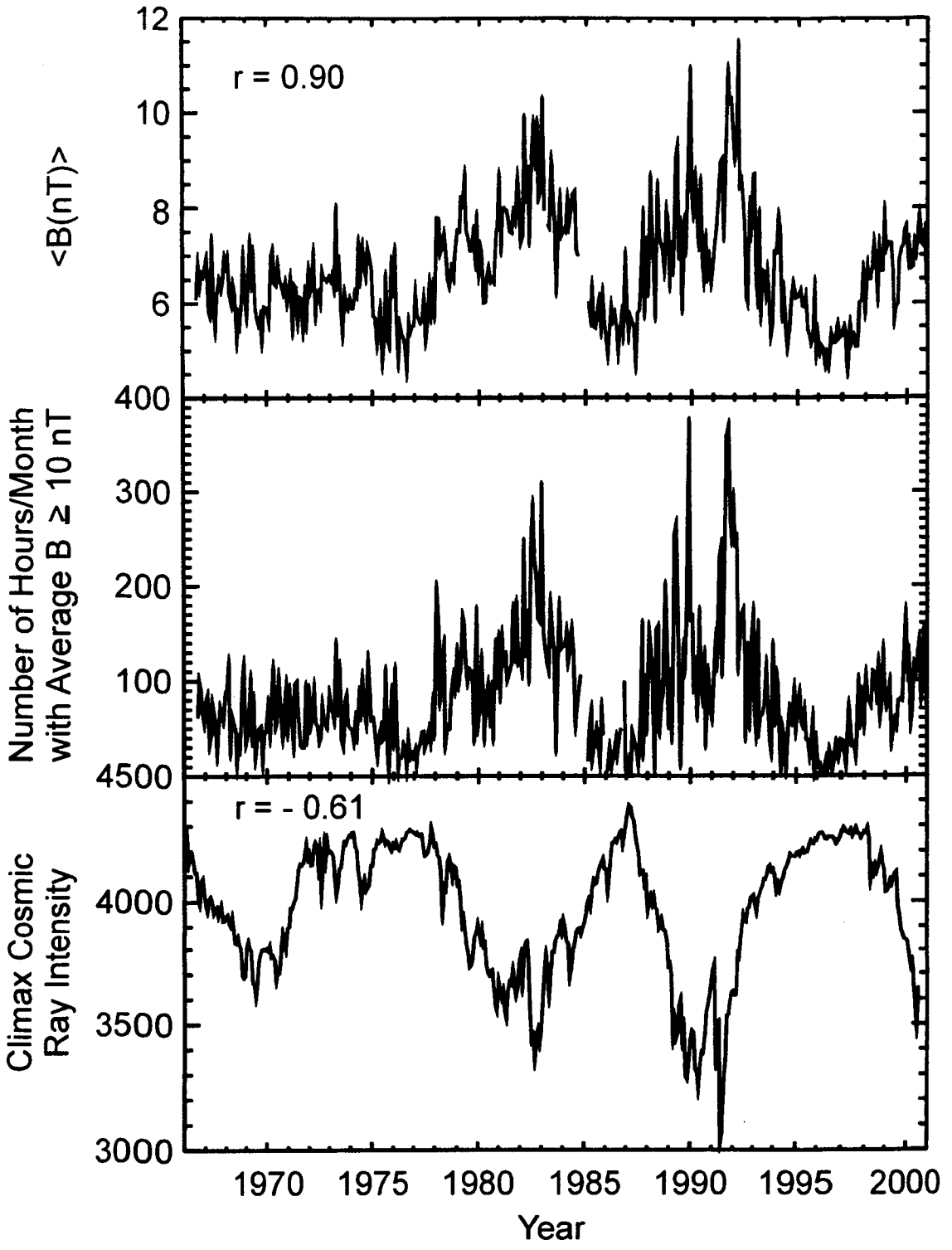
r = 0.90
<B(nT)>
12
10
8
6
400
300
200
100
Number of Hours/Month
with Average B ≥ 10 nT
4500
r = - 0.61
4000
3500
3000
Climax Cosmic
Ray Intensity
1970
1975
1980
1985
1990
1995
2000
Year

Figure 6